Toward Designing Highly Conductive Polymer Electrolytes by Machine Learning Assisted Coarse-Grained Molecular Dynamics

Yanming Wang,*,[⊥] Tian Xie,[⊥] Arthur France-Lanord, Arthur Berkley, Jeremiah A. Johnson, Yang Shao-Horn, and Jeffrey C. Grossman*

Read Online

ACCESS | Metrics & More | Article Recommendations | Supporting Information

ABSTRACT: Solid polymer electrolytes (SPEs) are considered promising building blocks of next-generation lithium-ion batteries due to their advantages in safety, cost, and flexibility. However, current SPEs suffer from a low ionic conductivity, motivating the development of novel highly conductive SPE materials. Here we propose a new SPE design approach that integrates coarse-grained molecular dynamics (CGMD) with machine learning. A continuous high-dimensional design space, composed of physically interpretable universal descriptors, was constructed by the coarse graining of chemical species. A Bayesian optimization (BO) algorithm was then employed to efficiently explore this space via autonomous CGMD simulations. Adopting this CGMD-BO approach, we obtained comprehensive descriptions of the relationships between the lithium conductivity and intrinsic material properties at the molecular level, such as the molecule size and nonbonding interaction strength, to provide guidance on directions to improve upon the components of the best-known electrolytes, including anion, secondary site, and backbone chain.
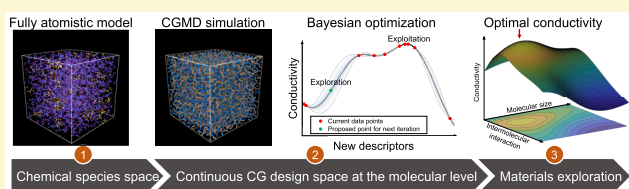
INTRODUCTION

Lithium-ion batteries have been applied in a wide range of applications, from personal devices to grid scale energy storage.[1] In pursuit of safer and more durable lithium-ion batteries at lower cost, solid polymer electrolytes (SPEs) are promising building blocks due to their unique advantages such as absence of flammable solvents, compatibility with roll-to-roll processes, and intrinsic flexibility and stretchability.[2,3] However, the low ionic conductivity of current SPEs prevents their further incorporation into real-world applications.[4] This challenge motivates tremendous research efforts toward the design of highly conductive SPE materials[2,5−7] via investigating the ionic transport mechanisms[8,9] and exploring candidate SPE materials[10,11] (where simulations and modeling have already made valuable contributions[12,13]). With the recent rapid development of artificial intelligence (AI),[14] machine learning (ML) techniques have started to play roles in improving and reforming the design loop of SPE materials.[10,11,15] AI and ML developments provide immense opportunities to examine molecular moieties in polymer electrolytes and correlate their dynamics and energetics with ion transport properties. To fully understand what governs the ion mobility and achieve global optimization of the SPE system, the identification of universally applicable descriptors is of great importance, but this is very difficult in a typical design space constructed by chemical species. Besides, in the case of SPEs, the complexity of the system, which mixes long chain polymers and lithium compounds, places it beyond the capacity of conventional fully atomistic (FA) simulations as a means to generate data sets

with the sizes suitable for many popular ML algorithms (e.g., a training data set containing $10^4−10^5$ samples is usually preferred[16]).

In this work, we propose a new framework for design of SPE materials that combines coarse-grained molecular dynamics (CGMD) with Bayesian optimization (BO). In addition to a great reduction in the computational cost, the CG simulation also preserves molecular level information, converting the discrete chemical species space to a continuous space constructed by the CGMD parameters. The adoption of the BO algorithm enables efficient exploration of this high-dimensional design space. From this, we can predict the relationships between the associated molecular level material properties (e.g., molecule sizes and intermolecular interactions) and the electrolyte performance to gain useful mechanistic insights and optimize SPE functions.
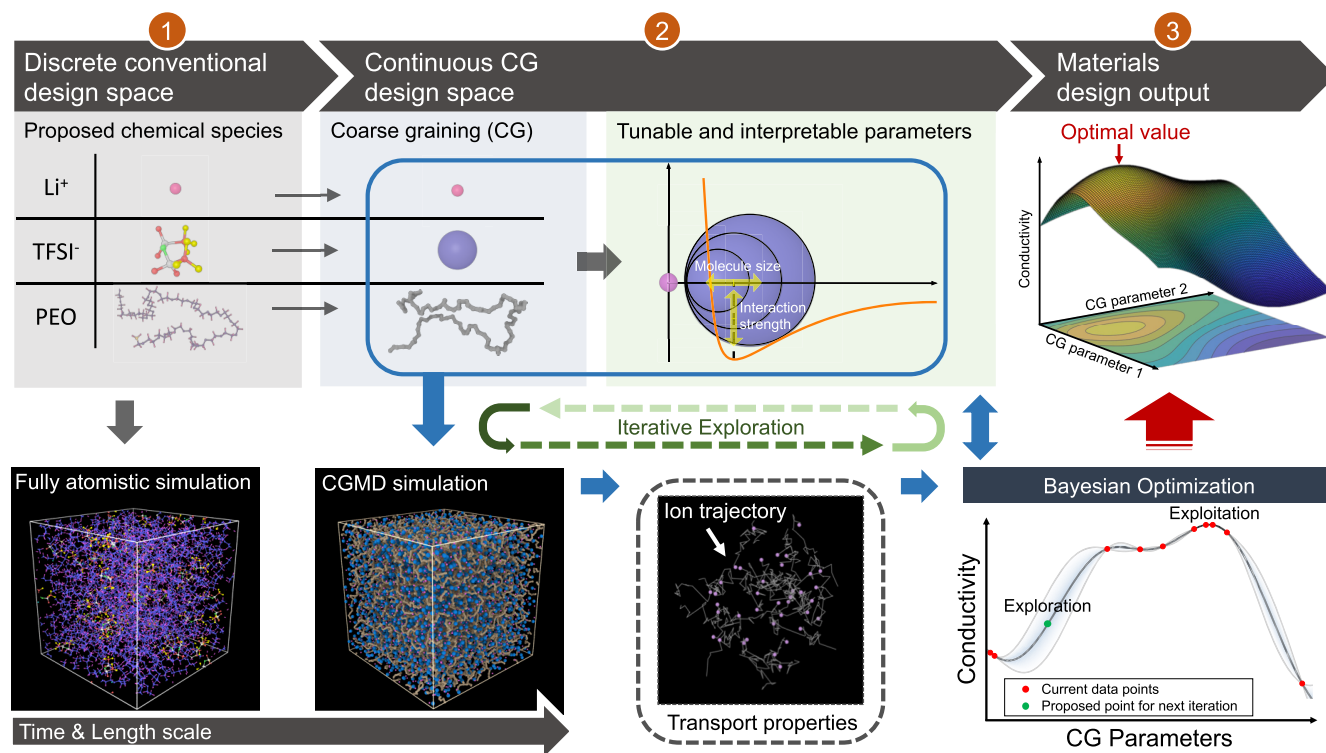
To train the CGMD-BO model, we first construct a design space using a set of CGMD parameters, including the molecule sizes and intermolecular interaction strengths, that completely define the properties of our designated "improvable components" in a SPE system, specifically the anions, backbone chains, and possible secondary sites (e.g., by
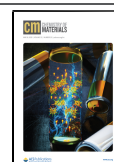
Figure 1. Illustration of the coarse-grained molecular dynamics−Bayesian optimization (CGMD-BO) framework. Materials design starts with the coarse-graining process to transform the conventional chemical species space to a continuous space composed of CG parameters (① → ②). This space is then explored by BO-guided CGMD simulations in iterations to predict the relationships between the transport properties and the associated CG parameters (② → ③).

introducing chemical variations in PEO chains[17]). In this CG space, we set the starting point of our exploration at the parameters that represent the poly(ethylene oxide)−lithium bis(trifluoromethanesulfonyl)imide (PEO−LiTFSI) system, considering that the PEO−LiTFSI exhibits the highest conductivity among the SPE candidates that have been extensively studied.[6,18] Once the CG space is constructed, we then aim to optimize the lithium ionic conductivity σ_{Li^+}, by an iterative parallel BO training process. The learned CGMD-BO model provides a detailed description of the relationships between the σ_{Li^+} and the CGMD parameters, from which we propose the directions and principles for changing TFSI−, introducing secondary sites, and replacing PEO backbone chains.

RESULTS

Figure 1 demonstrates the concept of the SPE materials design pathway via BO-guided CGMD simulations. Conventionally, computation guided materials design starts with the proposal of a set of chemical species. These serve as the inputs to fully atomistic (FA) simulations to obtain a detailed and accurate description of the system. However, considering the time and length scale limitations of the FA models (for example, a typical 10 ns classical MD run for one PEO/LiTFSI system with 20000 atoms requires 1500 CPU hours on an Intel Xeon Gold core), we propose an alternative coarse-graining (CG) process that abstracts the polymer chains and the anion molecules with a bead−spring representation.[19] Compared to the FA model, the CG configuration maintains most of the capability to capture the polymer conformation, while using fewer particles in the simulation cell to reduce the computa-

tional cost. Through the CG process, molecular level information such as molecular size and intermolecular interaction strength become CGMD parameters. Calibration of the CG system by the FA model (details in the Methods section, Figures S2 and S3) provides the values of these parameters for a desired electrolyte system (e.g., PEO−LiTFSI) and also accomplishes the transformation from a discrete conventional design space to a continuous CG design space.

The CGMD simulation defines a function f that maps from the continuous CG design space to the performance of the SPE material. Given a set of input parameters, the CGMD simulation generates the trajectory of the particles, from which the transport properties such as the ionic conductivity and the transference number can be extracted to compute performance metrics for the corresponding SPE material. We can thus reformulate our goal as to find the set of input parameters, i.e., the SPE material, that maximizes the performance metrics.

As illustrated in Figure 1, to efficiently explore the continuous CG design space and maximize the performance of SPE materials, we design a Bayesian optimization (BO) approach that utilizes the information from past simulations iteratively. In each iteration, we compute the a posterior estimation of the target function $p(f|\mathcal{D}_0), ..., \mathcal{D}_i$ using all previous simulation data and propose the next points in the CG design space as inputs to CGMD by balancing exploration and exploitation. By the end of this process, the model outputs a posterior estimation of the objective function $p(f|\mathcal{D})$ from which the optimal lithium conductivity and its dependences on all the input CGMD parameters can be extracted. Compared with existing works that use BO in materials design,[20−22] our
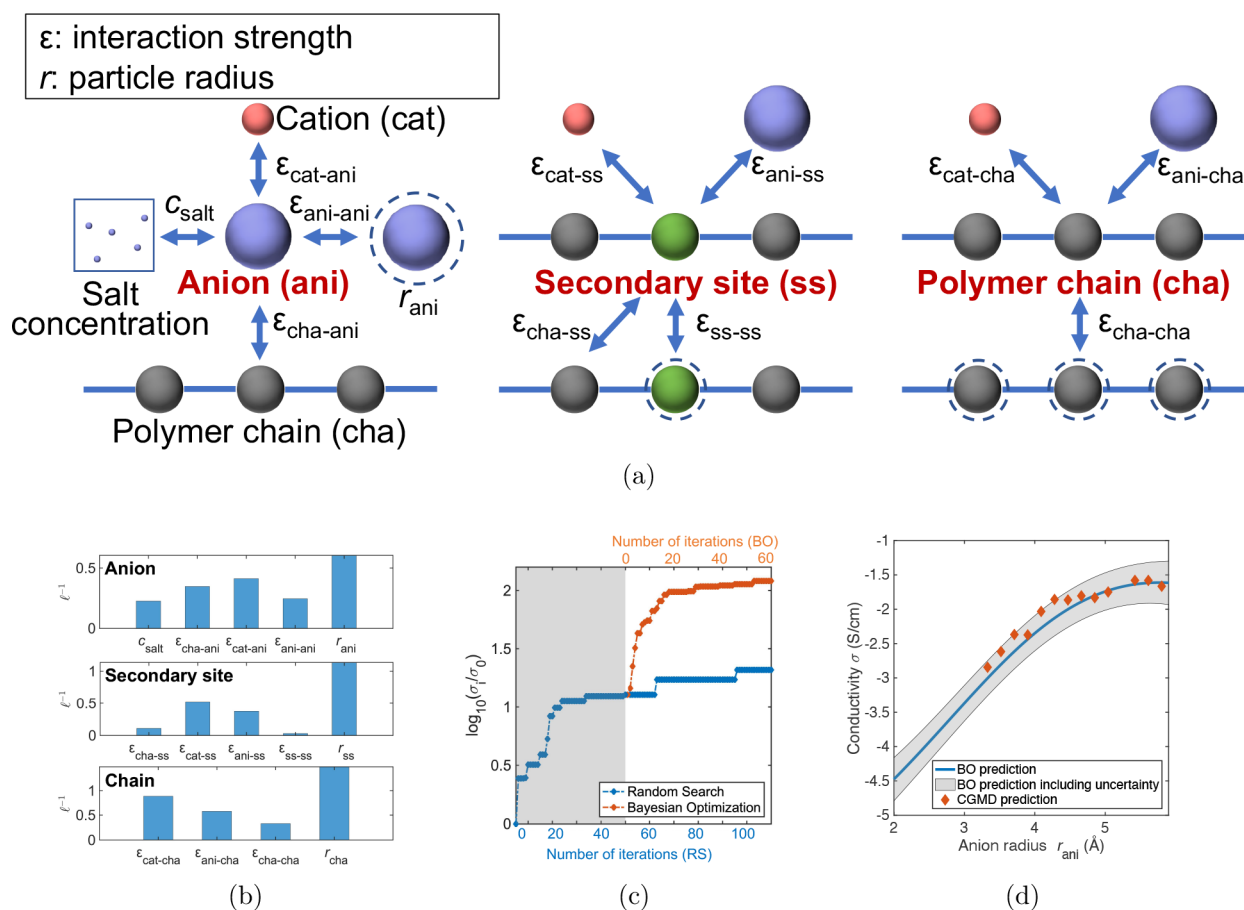
Figure 2. Evaluation of the Bayesian optimization training process. (a) Illustration of the CGMD parameters, which are divided into three groups for describing the properties associated with the anions, secondary sites, and backbone chains (from left to right), (b) the inverse of characteristic length scale for each CGMD parameter in the BO training process, (c) the design space exploration efficiency of BO in comparison with random search, and (d) the BO predicted conductivities in comparison with the CGMD test data.

approach uses several key characteristics of the system to improve the efficiency further: (1) adopting the local penalization algorithm,[23] multiple points are proposed in each iteration to better utilize the parallel computation of modern super computers; (2) the continuity of f and the intrinsic noise of CGMD simulations are built into the BO model to provide a more reliable estimation of f.

In the practice of the above design method, as demonstrated in Figure 2a, we divide all the designated independent CGMD parameters into three categories: five related to the properties of the anions (anion size, salt concentration, and anion involved vdW interaction strengths), five related to the properties of the secondary sites introduced in the polymer chain (molecule size and secondary site involved nonbonding interaction strengths), and four to determine the properties of the polymer chain itself (monomer size and polymer involved nonbonding interaction strengths). This division naturally sets up three exploration directions in the CG design space, corresponding to modifications to the anions, the secondary sites, and the polymer backbone chains. The search range of these parameters is determined based on their values of the reference PEO−LiTFSI system, with the lower and upper bounds capped by their physical interpretations, e.g., typically the vdW interaction strength $\epsilon_{ij} \in (0.4, 6)$ kcal/mol and the particle radius $r_i \in (1.5, 5)$ Å. Specifically, we set the target property of the materials optimization to the lithium conductivity σ_{Li^+}, which is defined as the product of the

overall conductivity σ and the lithium transference number t_{Li^+}. This setup enables our exploration to not only maximize σ but also put emphasis on t_{Li^+}, considering that increasing t_{Li^+} could effectively reduce the concentration polarization and improve the stability of the electrolyte system in the charge−discharge cycles.[9,24,25]

Figure 2b shows the inverse of characteristic length scale l^{-1} (a learned parameter in the BO model) of each CG parameter, which can be considered as a measure of the parameter importance in the BO training process. A larger l^{-1} indicates that the change of this parameter will be likely to make more impact on σ_{Li^+}. (l^{-1} only reflects the average effect of each CG parameter on σ_{Li^+} for the entire design space we explore. Thus, it is possible that the parameter with the highest l^{-1} may not be the most influential factor for search in some subspaces.) In all three explorations, the size of the particle was found to be the most influential factor, while the interaction strength associated with the cation ranked second. In contrast, the role of the interchain interaction was not crucial, possibly because its strength was small compared to other interactions involving charged particles.

To compare the searching efficiency of the BO method with a random search (RS), Figure 2c plots the normalized best-so-far (BSF) conductivity as a function of the iteration number, where for RS the BSF value plateaus after around 50 random explorations. In contrast, given a RS-generated initial data set
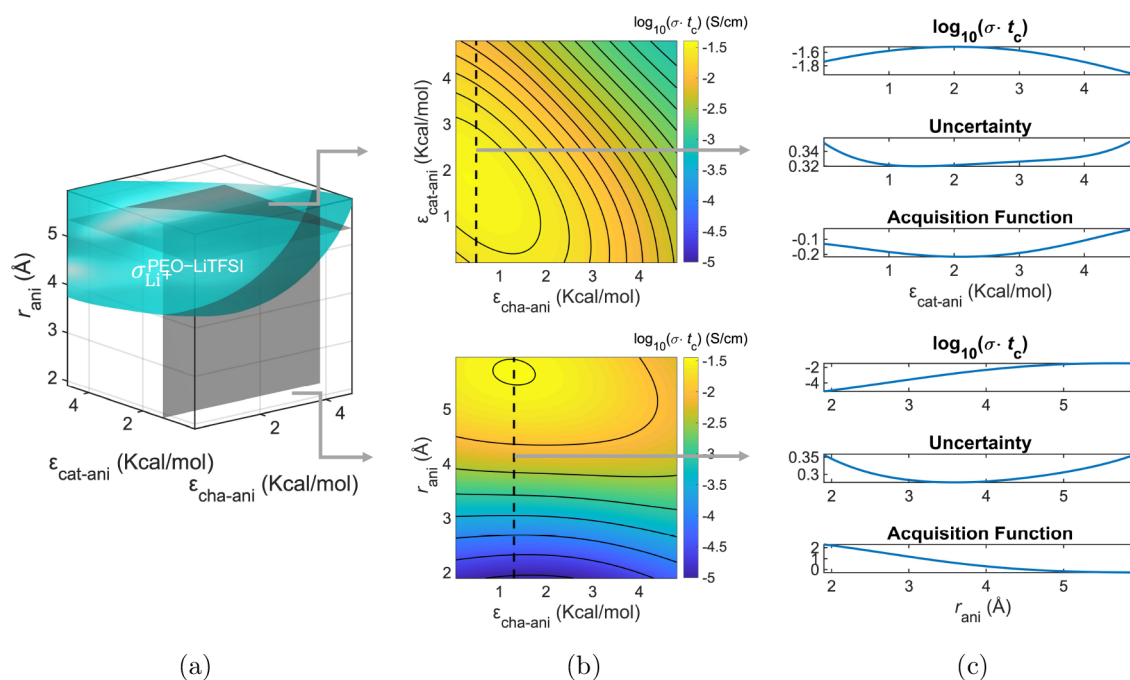
Figure 3. Anion effects on lithium conductivity. (a) 3D isosurface plot at the lithium conductivity value of PEO−LiTFSI, (b) 2D σ_{Li^+} landscape projected in $\varepsilon_{cat-ani}−\varepsilon_{cha-ani}$ and $r_{ani}−\varepsilon_{cha-ani}$ planes, and (c) 1D cross-sectional plots showing the dependence of σ_{Li^+} on $\varepsilon_{cat-ani}$ and r_{ani}, with the uncertainty evaluations and the acquisition function values.

with the size of 50, the BO improves the BSF values more efficiently and converges to a much higher conductivity within only around 60 iterations; i.e., to reach the same BSF value, the RS method will take a much longer time. This result indicates that the CGMD-BO method is an efficient approach for SPE materials optimization. To validate the model, a test data set was built, containing the conductivities calculated from a series of CGMD simulations performed at different anion sizes (with the other parameters kept the same as the reference PEO−LiTFSI system). As shown in Figure 2d, both the values and the trend presented by these test data were well reproduced by the trained BO model. It should be noted that the agreement was achieved under the condition that the BO model used only around 100 sampling points to search this high-dimensional CG space, and none of these training data were close to the test data in the design space.

The CGMD-BO model was adopted to investigate the consequences of possible modifications to the anions on the lithium conductivity σ_{Li^+}. The obtained relation between σ_{Li^+} and the most influential three anion-related parameters ($\varepsilon_{cat-ani}$, $\varepsilon_{cha-ani}$, and r_{ani}, referring to Figure 2b) is described in Figure 3a, in the form of an isosurface plot at the σ_{Li^+} value of the reference PEO−LiTFSI system ($\sim10^{-3}$ S/cm[26]). In Figure 3b, at a fixed anion radius, a 2D landscape is drawn to describe σ_{Li^+} as a function of $\varepsilon_{cat-ani}$ and $\varepsilon_{cha-ani}$. In general, while a moderate value of $\varepsilon_{cha-ani}$ was necessary for dissolving the anions, if the $\varepsilon_{cha-ani}$ was too large, it would lead to the reduction of σ_{Li^+}, which could result from the increased population of polymer cross-linking through the anions. Also, the optimal value of $\varepsilon_{cha-ani}$ was found to be positively correlated to $\varepsilon_{cat-ani}$; namely, decreasing $\varepsilon_{cha-ani}$ and $\varepsilon_{cat-ani}$ together would be beneficial to the lithium conductivity, where an optimum value of $\varepsilon_{cat-ani}$ was needed to maximize σ_{Li^+}. At this $\varepsilon_{cat-ani}$, the repulsive contribution between the cation and the anion may be balanced with their attractive Coulombic interaction, effec-

tively lowering the ion dissociation energy in polymer (Figure S1). When we project σ_{Li^+} in the $r_{ani}−\varepsilon_{cha-ani}$ plane, a significant increase of σ_{Li^+} can be observed by increasing r_{ani} in most of the BO searching area, mainly due to the decaying Coulombic interaction at larger charge separation distance. This is consistent with the fact that in many cases a larger anion could enhance the delocalization of the negative charge.[27,28] (In our current CG model, the size increase of the anion inherently implies an effective higher degree of charge delocalization; however, it should be noted that this may not always be true in reality.) In opposition to the above positive relation between σ_{Li^+} and r_{ani}, a larger anion volume also introduces a more severe obstacle that suppresses the system diffusion. Therefore, on the σ_{Li^+} landscape there exists an optimal value of r_{ani}, which slightly decreases with stronger $\varepsilon_{cha-ani}$.

We also examined the σ_{Li^+} dependence on a single factor by cross sectioning the 2D landscape. For example, as shown in Figure 3c, we provide the curves representing the $\sigma_{Li^+}−\varepsilon_{cat-ani}$ and $\sigma_{Li^+}−r_{ani}$ relations, which further supports the above analysis. Figure 3c also gives the estimates of uncertainty (in the form of standard deviation), in conjunction with the BO acquisition function, whose value is proportional to the probability of the region that will be evaluated in the next iteration. Overall, the uncertainty fluctuates within a small range; thus, the minimum of the acquisition function (AF_{min}) occurs near the CGMD parameter value that tends to yield high σ_{Li^+}, leading to further exploitation of this region. On the other hand, at the beginning of the BO training, the AF_{min} may appear at the position where the uncertainty is relatively high to enforce the exploration of the entire parameter space.

The CGMD-BO method was also adopted to investigate the effects of introducing secondary sites (SS) to PEO chains on the lithium conductivity. For simplicity, setting the reference system to PEO−LiTFSI, we tuned the properties of SS while
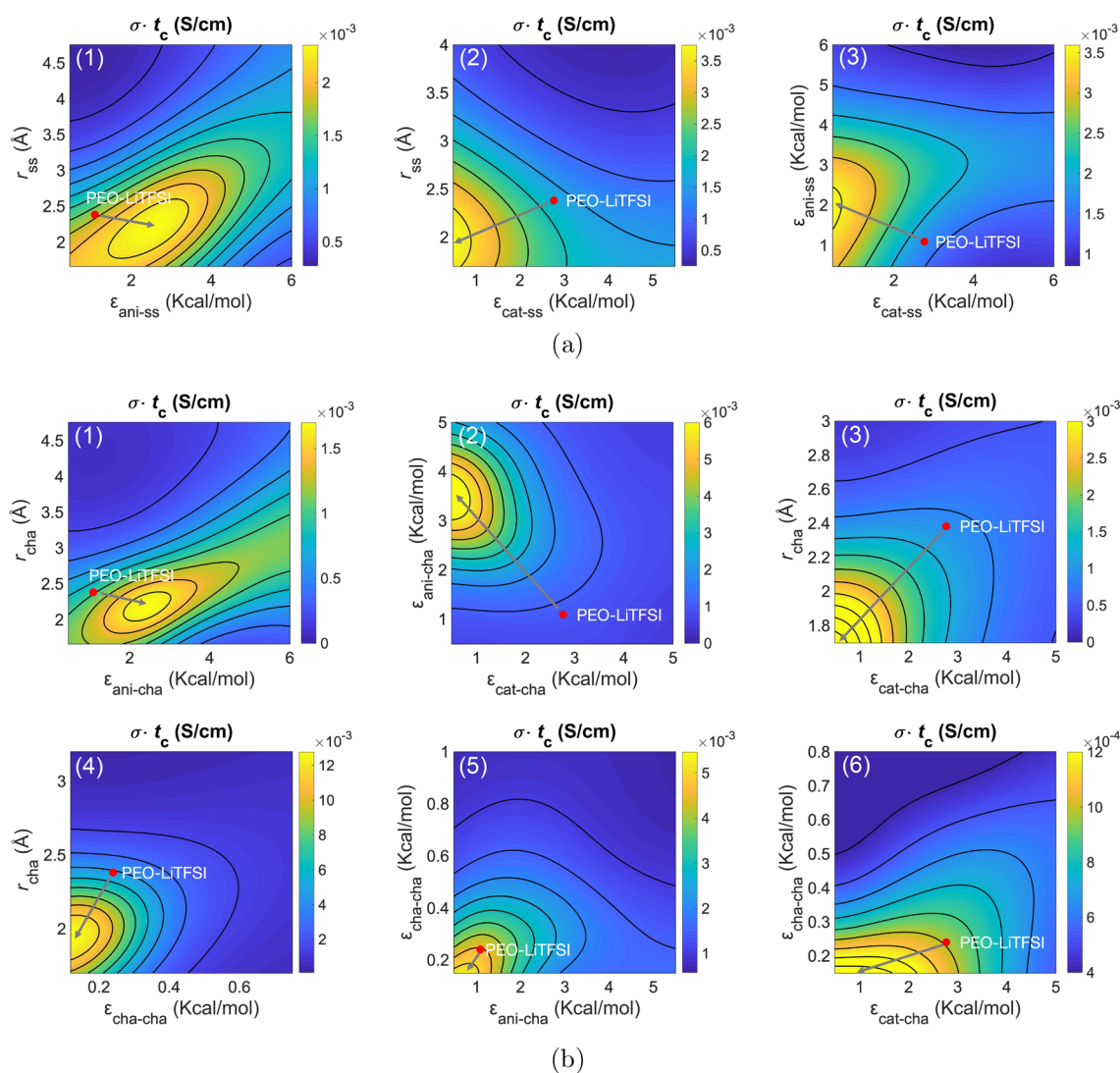
Figure 4. Effects of secondary sites and polymer backbone chains on lithium conductivity. A series of 2D σ_{Li^+} landscape plots for the materials exploration of (a) secondary sites and (b) polymer backbone chains. Each subfigure shows the dependence of σ_{Li^+} on a pair of CGMD parameters, with the other parameters fixed at the values of the reference PEO−LiTFSI system. The red dots on the graphs denote the reference PEO−LiTFSI system, with the arrows pointing out the directions to maximize σ_{Li^+}.

keeping the SS to EO ratio at 1/5. The model predictions were collected as a set of 2D σ_{Li^+} landscapes in Figure 4a. In each of the landscape plots, the lithium conductivity were contoured on a plane determined by a pair of CGMD parameters, with the red dot marking the position of the unmodified PEO−LiTFSI system. From Figure 4a, one can conclude that a promising SS is expected to have a size smaller but close to the EO monomer and a selective and modestly strong interaction with the anion. These properties enhance the cation diffusion and immobilize the anions. This is in opposition to the properties of PEO but in accordance with the rationale for the proposal of single lithium-ion conducting polymers in the literature.[27,28]

We noted that the improvement of σ_{Li^+} due to the introduction of SS, in comparison with unmodified PEO-LiTFSI, was rather limited. This inspired us to probe the possibility of designing non-PEO-based SPE materials, which is actually an active research direction where several novel non-PEO-based polymer architectures have been proposed and investigated experimentally.[29−33] Figure 4b presents the change of σ_{Li^+} induced by varying any two CGMD parameters

away from the PEO reference. Based on Figure 4b, favorable polymer candidates tend to shrink their sizes and weaken their interchain interaction (e.g., Figure 4b(4)), presumably to achieve high diffusivity and flexibility. In addition, as here we aim to maximize the conductivity contributed by the lithium ion, our CGMD-BO model consistently suggests the design direction of increasing $\varepsilon_{ani-cha}$ together with decreasing $\varepsilon_{cat-cha}$ to create more free Li$^+$ in the SPE system.[34] Even so, one may consider the negative effects of increasing $\varepsilon_{ani-cha}$ on chain diffusivity, which explains why there exists an optimal $\varepsilon_{ani-cha}$ (as shown in Figure 4b(1) and (2)).

■ DISCUSSION

The trained CGMD-BO model can be utilized as a rich SPE materials database. To obtain the transport properties of one specific SPE system, the model only requires a CG parametrization of the molecule species, through a set of straightforward energy evaluations by either all-atom force fields or DFT. In comparison with classical fully atomistic approaches that require days or even months to obtain

conductivity values, the CGMD-BO model reduces the time of the process down to minutes. For instance, without performing any additional simulations, as shown in Figure 5, the trained
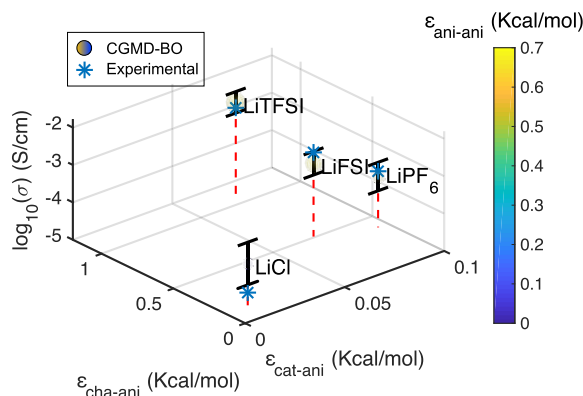
Figure 5. CGMD-BO predictions on conductivity for several common electrolyte systems. The trained BO model predicts conductivities for the PEO−LiTFSI, PEO−LiFSI, PEO−LiPF$_6$, and PEO−LiCl systems, which are plotted with the uncertainty information (shown as error bars) and their corresponding CG parameters, in comparison with experimental measurements (represented by asterisks).[18,26,35,36]

BO model predicts and compares the conductivities of four common electrolyte systems (the input parameters to the CGMD-BO model are shown in the plot and listed in Table S1) to reasonable agreement with the experimental measurements.[18,26,35,36] This suggests the potential of the CGMD-BO model as a convenient tool for rapid screening of the candidate materials prior to synthesis. Besides, Figure 5 shows that rather than being determined by a single factor, the change of conductivity is more likely to be a joint effect of all the molecular properties on this plot (e.g., anion size and the anion associated intermolecular interactions). This again implies the complexity of the SPE materials design space, which is almost impossible to be explored without the CGMD-BO approach.

In this work, using the molecular-level material properties as descriptors, the CGMD-BO framework has shown its unique advantages of efficiency and flexibility in the optimization of σ_{Li^+}. Furthermore, with minor modifications, the model can be extended to adopt additional descriptors from microstructural features (e.g., the Li-ion solvation-site connectivity[32]) to macroscopic material properties (e.g., polymer stiffness and glass transition temperature) to discover the correlations among the descriptors at different scales and their joint effects on the lithium conductivity. Broadly speaking, we expect the CGMD-BO framework to be a promising approach to understanding the collective effects of the molecular descriptors on a wide range of properties of a given system (not limited to the polymer−salt mixture) for the design of complex multicomponent material systems. So far, all the CG parameters are independently adjustable, enabling us to reach every corner of the design space. In reality, correlations usually exist among the parameters, confining the exploration to one or several subspaces of our current CG design space. In principle, these constraints could be better understood with data from the CG parametrization of more SPE materials. Besides, the process of the CG parametrization and the CG model itself could be more refined to further improve the prediction accuracy of the current CGMD-BO model. (For

example, the accuracy of the CG model could be improved by calibrating its parameters to FA simulations with a polarizable force field.[37] Taking the information about cation solvation-site structures and the distribution from FA trajectories, a dynamic bond percolation model could be adopted to further accelerate the CG simulations.[38]) Last, we anticipate that the CGMD-BO model can go beyond its current capability to make further contributions to new materials design. By taking advantage of machine learning to understand the structure−property relationships,[16] it progressively becomes achievable to recognize and decode the similarities between the micro-structural features of coarse-grained and fully atomistic models.[39] We believe that the joint efforts from more advanced ML algorithms, more accurate CG models, and sufficient training data should ultimately achieve the recovery of the atomistic details from molecular level information, which will grant the CGMD-BO method the ability to propose chemical species directly.

■ METHODS

Coarse-Grained Molecular Dynamics. The CGMD simulations are performed by using the Large-scale Atomic/Molecular Massively Parallel Simulator (LAMMPS).[40] The functional form of the Class2 force field[41] is taken to describe the bonding interactions. To account for the nonbonding interactions, the Lennard-Jones 12−6 potential plus the Coulombic term is adopted, with the PPPM method for long-range Coulombic interactions.[42] To obtain the CGMD parameters for the PEO−LiTFSI reference system (values of the parameters in Table S2), fully atomistic data are generated through a series of static energy evaluations. All-atom calculations were also performed by using LAMMPS,[40] as implemented in the MedeA simulation environment. The interatomic interactions were modeled by using the Polymer Consistent Force-Field (PCFF+).[41] This force field has already been used to model PEO/LiTFSI electrolytes[43] before. For parametrizing each pair interaction, as demonstrated in Figure S2, two prerelaxed molecules were constrained at 200 different center-of-mass distances. At each fixed distance, the intermolecular energies (excluding the contributions from long-range Coulombic interactions for charged molecules) were evaluated and then averaged for 1260 different molecular orientations to obtain the average energy−distance relations. These data were used to fit the parameters of the Lennard-Jones equation by using the damped least-squares (DLS) method[44] with a tolerance of 10^{-6} kcal/mol, which yielded the results in Figure S3.

A typical CG initial configuration consists of 100 random placed polymer chains, with 100 monomers per chain. Setting a default salt to monomer ratio to 1/10, 1000 Li$^+$ cations with the same number of counterions are inserted into the system (Figure S4a). Each CGMD simulation starts with the initial equilibration by a two-step protocol to reach the conformational equilibrium (Figure S4b),[45] followed by a 10 million steps simulation with the time step of 1 fs at 80 °C under the NVT ensemble. From the simulation trajectory, the ionic conductivity is extracted by the Green−Kubo (GK) relation, as the conventional Nernst−Einstein equation is not valid in the high salt concentration regime. The velocity autocorrelation functions for the ions are calculated for a period of 1500 ps (Figure S5b). Considering that the conductivity derived from the GK approach is typically with large noises (Figure S5c), the time average is taken by using the conductivity data after 100 ps to improve the reliability of the conductivity prediction. (For instance, as shown in Figure S5d, the fluctuation of the time-averaged conductivity is much smaller, and a convergence is likely to be achieved at around 1 ns.) The transference number is estimated by calculating the self-diffusivities of the cations and anions from fitting the linear regimes in the mean-square displacement curves (Figure S5a). We aware that this conventional definition of transference number may cause an overestimate for polymer electrolyte in the high salt concentration regime due to

significant ion-pairing effects. However, as the salt concentration was kept constant for all the data presented in this paper, we expect that the correlations discovered by the CGMD-BO approach should still preserve. For future study, more sophisticated methods for the transference number calculation[17,46,47] can be incorporated into our framework. As the current CGMD model already has the ability to qualitatively reproduce the experimental relationship between salt concentration and conductivity for the PEO−LiTFSI system (Figure S6), with adopting a more refined definition of transference number, the accuracy of the model prediction can be further improved.

Bayesian Optimization. Bayesian optimization (BO)[48] is a systematic approach to find the minimum or maximum of an unknown function $f: \mathbb{R}^D \to \mathbb{R}$, where the gradient of f is unknown and the evaluation of f is expensive. In this study, f is the CGMD simulation with the input space being the CG design space and the output space being the target material property. The BO includes the following steps: (1) Select a prior for the possible space of function f. (2) Compute the posterior given the prior and current simulation data. (3) Use the posterior to decide the next point to evaluate according to an acquisition function. (4) Run the simulation to obtain data. Steps 2−4 are iterated to explore the CG design space until convergence.

In this study, we employ a Gaussian process prior with a Matern 5/2 kernel[48] to measure the continuity of f, and we added a Gaussian noise on the target value to account for the intrinsic noise of CGMD simulations. In each iteration, we use a lower confidence bound acquisition function to decide the next points to evaluate and employ the local penalization method[23] to make multiple evaluations in a single iteration. The code is modified on top of the open-source library GPyOpt.[49]

■ ASSOCIATED CONTENT

ⓈⒾ Supporting Information

The Supporting Information is available free of charge at https://pubs.acs.org/doi/10.1021/acs.chemmater.9b04830.

> Relationship between the cation−anion interaction and the parameter $\varepsilon_{cat-ani}$, configuration of the fully atomistic calculations for CG force field parametrization, intermolecular distance−average energy relationship, equilibrated polymer configuration, details of the lithium conductivity calculations, relationship between the conductivity and the salt-to-monomer ratio, the CGMD parameters of several anion species, and the CGMD parameters of the PEO−LiTFSI system (PDF)

■ AUTHOR INFORMATION

Corresponding Authors

Yanming Wang − *Department of Materials Science and Engineering, Massachusetts Institute of Technology, Cambridge, Massachusetts 02139, United States;* ⓞ orcid.org/0000-0002-0912-681X; Email: yanmingw@mit.edu

Jeffrey C. Grossman − *Department of Materials Science and Engineering, Massachusetts Institute of Technology, Cambridge, Massachusetts 02139, United States;* ⓞ orcid.org/0000-0003-1281-2359; Email: jcg@mit.edu

Authors

Tian Xie − *Department of Materials Science and Engineering, Massachusetts Institute of Technology, Cambridge, Massachusetts 02139, United States;* ⓞ orcid.org/0000-0002-0987-4666

Arthur France-Lanord − *Department of Materials Science and Engineering, Massachusetts Institute of Technology, Cambridge, Massachusetts 02139, United States;* ⓞ orcid.org/0000-0003-0586-1945

Arthur Berkley − *Department of Materials, Oxford University, Oxford OX1 2JD, U.K.*

Jeremiah A. Johnson − *Department of Chemistry, Massachusetts Institute of Technology, Cambridge, Massachusetts 02139, United States;* ⓞ orcid.org/0000-0001-9157-6491

Yang Shao-Horn − *Department of Mechanical Engineering, Massachusetts Institute of Technology, Cambridge, Massachusetts 02139, United States;* ⓞ orcid.org/0000-0001-8714-2121

Complete contact information is available at:
https://pubs.acs.org/10.1021/acs.chemmater.9b04830

Author Contributions

Notes

The authors declare no competing financial interest.

■ ACKNOWLEDGMENTS

■ REFERENCES

(1) Dunn, B.; Kamath, H.; Tarascon, J.-M. Electrical energy storage for the grid: a battery of choices. *Science* **2011**, *334*, 928−935.

(2) Agrawal, R.; Pandey, G. Solid polymer electrolytes: materials designing and all-solid-state battery applications: an overview. *J. Phys. D: Appl. Phys.* **2008**, *41*, 223001.

(3) Li, L.; Lou, Z.; Chen, D.; Jiang, K.; Han, W.; Shen, G. Recent advances in flexible/stretchable supercapacitors for wearable electronics. *Small* **2018**, *14*, 1702829.

(4) Blomgren, G. E. The development and future of lithium ion batteries. *J. Electrochem. Soc.* **2017**, *164*, A5019−A5025.

(5) Tikekar, M. D.; Choudhury, S.; Tu, Z.; Archer, L. A. Design principles for electrolytes and interfaces for stable lithium-metal batteries. *Nat. Energy* **2016**, *1*, 16114.

(6) Yue, L.; Ma, J.; Zhang, J.; Zhao, J.; Dong, S.; Liu, Z.; Cui, G.; Chen, L. All solid-state polymer electrolytes for high-performance lithium ion batteries. *Energy Storage Materials* **2016**, *5*, 139−164.

(7) Miller, T. F., III; Wang, Z.-G.; Coates, G. W.; Balsara, N. P. Designing polymer electrolytes for safe and high capacity rechargeable lithium batteries. *Acc. Chem. Res.* **2017**, *50*, 590−593.

(8) Maitra, A.; Heuer, A. Cation transport in polymer electrolytes: A microscopic approach. *Phys. Rev. Lett.* **2007**, *98*, 227802.

(9) Chintapalli, M.; Timachova, K.; Olson, K. R.; Mecham, S. J.; Devaux, D.; DeSimone, J. M.; Balsara, N. P. Relationship between conductivity, ion diffusion, and transference number in perfluoropolyether electrolytes. *Macromolecules* **2016**, *49*, 3508−3515.

(10) Mannodi-Kanakkithodi, A.; Chandrasekaran, A.; Kim, C.; Huan, T. D.; Pilania, G.; Botu, V.; Ramprasad, R. Scoping the polymer genome: A roadmap for rational polymer dielectrics design and beyond. *Mater. Today* **2018**, *21*, 785−796.

(11) Hatakeyama-Sato, K.; Tezuka, T.; Nishikitani, Y.; Nishide, H.; Oyaizu, K. Synthesis of Lithium-ion Conducting Polymers Designed by Machine Learning-based Prediction and Screening. *Chem. Lett.* **2019**, *48*, 130.

(12) Borodin, O.; Smith, G. D. Mechanism of ion transport in amorphous poly (ethylene oxide)/LiTFSI from molecular dynamics simulations. *Macromolecules* **2006**, *39*, 1620−1629.

(13) Mogurampelly, S.; Borodin, O.; Ganesan, V. Computer simulations of ion transport in polymer electrolyte membranes. *Annu. Rev. Chem. Biomol. Eng.* **2016**, *7*, 349−371.

(14) Butler, K. T.; Davies, D. W.; Cartwright, H.; Isayev, O.; Walsh, A. Machine learning for molecular and materials science. *Nature* **2018**, *559*, 547.

(15) Ahmad, Z.; Xie, T.; Maheshwari, C.; Grossman, J. C.; Viswanathan, V. Machine Learning Enabled Computational Screening of Inorganic Solid Electrolytes for Suppression of Dendrite Formation in Lithium Metal Anodes. *ACS Cent. Sci.* **2018**, *4*, 996−1006.

(16) Xie, T.; Grossman, J. C. Crystal Graph Convolutional Neural Networks for an Accurate and Interpretable Prediction of Material Properties. *Phys. Rev. Lett.* **2018**, *120*, 145301.

(17) France-Lanord, A.; Wang, Y.; Xie, T.; Johnson, J. A.; Shao-Horn, Y.; Grossman, J. C. The effect of chemical variations in the structure of poly (ethylene oxide)-based polymers on lithium transport in concentrated electrolytes. *Chem. Mater.* **2020**, *32*, 121.

(18) Gorecki, W.; Jeannin, M.; Belorizky, E.; Roux, C.; Armand, M. Physical properties of solid polymer electrolyte PEO (LiTFSI) complexes. *J. Phys.: Condens. Matter* **1995**, *7*, 6823.

(19) Underhill, P. T.; Doyle, P. S. On the coarse-graining of polymers into bead-spring chains. *J. Non-Newtonian Fluid Mech.* **2004**, *122*, 3−31.

(20) Balachandran, P. V.; Xue, D.; Theiler, J.; Hogden, J.; Lookman, T. Adaptive strategies for materials design using uncertainties. *Sci. Rep.* **2016**, *6*, 19660.

(21) Seko, A.; Togo, A.; Hayashi, H.; Tsuda, K.; Chaput, L.; Tanaka, I. Prediction of low-thermal-conductivity compounds with first-principles anharmonic lattice-dynamics calculations and Bayesian optimization. *Phys. Rev. Lett.* **2015**, *115*, 205901.

(22) Ju, S.; Shiga, T.; Feng, L.; Hou, Z.; Tsuda, K.; Shiomi, J. Designing nanostructures for phonon transport via Bayesian optimization. *Phys. Rev. X* **2017**, *7*, No. 021024.

(23) González, J.; Dai, Z.; Hennig, P.; Lawrence, N. Batch Bayesian optimization via local penalization. *Artificial Intelligence and Statistics*; 2016; pp 648−657.

(24) Shah, D. B.; Olson, K. R.; Karny, A.; Mecham, S. J.; DeSimone, J. M.; Balsara, N. P. Effect of anion size on conductivity and transference number of perfluoroether electrolytes with lithium salts. *J. Electrochem. Soc.* **2017**, *164*, A3511−A3517.

(25) Pesko, D. M.; Timachova, K.; Bhattacharya, R.; Smith, M. C.; Villaluenga, I.; Newman, J.; Balsara, N. P. Negative transference numbers in poly (ethylene oxide)-based electrolytes. *J. Electrochem. Soc.* **2017**, *164*, E3569−E3575.

(26) Zhang, H.; Liu, C.; Zheng, L.; Xu, F.; Feng, W.; Li, H.; Huang, X.; Armand, M.; Nie, J.; Zhou, Z. Lithium bis (fluorosulfonyl) imide/ poly (ethylene oxide) polymer electrolyte. *Electrochim. Acta* **2014**, *133*, 529−538.

(27) Ma, Q.; et al. Single lithium-ion conducting polymer electrolytes based on a super-delocalized polyanion. *Angew. Chem., Int. Ed.* **2016**, *55*, 2521−2525.

(28) Zhang, H.; Li, C.; Piszcz, M.; Coya, E.; Rojo, T.; Rodriguez-Martinez, L. M.; Armand, M.; Zhou, Z. Single lithium-ion conducting solid polymer electrolytes: advances and perspectives. *Chem. Soc. Rev.* **2017**, *46*, 797−815.

(29) Lee, Y.-C.; Ratner, M. A.; Shriver, D. F. Ionic conductivity in the poly (ethylene malonate)/lithium triflate system. *Solid State Ionics* **2001**, *138*, 273−276.

(30) Zhang, Z.; Jin, J.; Bautista, F.; Lyons, L.; Shariatzadeh, N.; Sherlock, D.; Amine, K.; West, R. Ion conductive characteristics of cross-linked network polysiloxane-based solid polymer electrolytes. *Solid State Ionics* **2004**, *170*, 233−238.

(31) Tominaga, Y.; Shimomura, T.; Nakamura, M. Alternating copolymers of carbon dioxide with glycidyl ethers for novel ion-conductive polymer electrolytes. *Polymer* **2010**, *51*, 4295−4298.

(32) Webb, M. A.; Jung, Y.; Pesko, D. M.; Savoie, B. M.; Yamamoto, U.; Coates, G. W.; Balsara, N. P.; Wang, Z.-G.; Miller, T. F., III Systematic computational and experimental investigation of lithium-ion transport mechanisms in polyester-based polymer electrolytes. *ACS Cent. Sci.* **2015**, *1*, 198−205.

(33) Zhao, Q.; Liu, X.; Stalin, S.; Khan, K.; Archer, L. A. Solid-state polymer electrolytes with in-built fast interfacial transport for secondary lithium batteries. *Nature Energy* **2019**, *4*, 365−373.

(34) Savoie, B. M.; Webb, M. A.; Miller, T. F., III Enhancing cation diffusion and suppressing anion diffusion via Lewis-acidic polymer electrolytes. *J. Phys. Chem. Lett.* **2017**, *8*, 641−646.

(35) Yang, X.; Lee, H.; Xiang, C.; McBreen, J.; Choi, L.; Okamoto, Y. Ion pair dissociation effects of aza-based anion receptors on lithium salts in polymer electrolytes; The Office of Scientific and Technical Information: Oak Ridge, TN, 1996.

(36) Ibrahim, S.; Yasin, S. M. M.; Nee, N. M.; Ahmad, R.; Johan, M. R. Conductivity, thermal and infrared studies on plasticized polymer electrolytes with carbon nanotubes as filler. *J. Non-Cryst. Solids* **2012**, *358*, 210−216.

(37) Borodin, O. Polarizable force field development and molecular dynamics simulations of ionic liquids. *J. Phys. Chem. B* **2009**, *113*, 11463−11478.

(38) Webb, M. A.; Savoie, B. M.; Wang, Z.-G.; Miller, T. F., III Chemically specific dynamic bond percolation model for ion transport in polymer electrolytes. *Macromolecules* **2015**, *48*, 7346−7358.

(39) Gómez-Bombarelli, R.; Wei, J. N.; Duvenaud, D.; Hernández-Lobato, J. M.; Sánchez-Lengeling, B.; Sheberla, D.; Aguilera-Iparraguirre, J.; Hirzel, T. D.; Adams, R. P.; Aspuru-Guzik, A. Automatic chemical design using a data-driven continuous representation of molecules. *ACS Cent. Sci.* **2018**, *4*, 268−276.

(40) Plimpton, S. Fast parallel algorithms for short-range molecular dynamics. *J. Comput. Phys.* **1995**, *117*, 1−19.

(41) Sun, H. Force field for computation of conformational energies, structures, and vibrational frequencies of aromatic polyesters. *J. Comput. Chem.* **1994**, *15*, 752−768.

(42) Hockney, R. W.; Eastwood, J. W. *Computer simulation using particles*; CRC Press: Boca Raton, FL, 1988.

(43) France-Lanord, A.; Grossman, J. C. Correlations from Ion Pairing and the Nernst-Einstein Equation. *Phys. Rev. Lett.* **2019**, *122*, 136001.

(44) Levenberg, K. A method for the solution of certain non-linear problems in least squares. *Q. Appl. Math.* **1944**, *2*, 164−168.

(45) Sliozberg, Y. R.; Andzelm, J. W. Fast protocol for equilibration of entangled and branched polymer chains. *Chem. Phys. Lett.* **2012**, *523*, 139−143.

(46) McDaniel, J. G.; Son, C. Y. Ion correlation and collective dynamics in BMIM/BF4-based organic electrolytes: from dilute solutions to the ionic Liquid Limit. *J. Phys. Chem. B* **2018**, *122*, 7154−7169.

(47) Fong, K. D.; Self, J.; Diederichsen, K. M.; Wood, B. M.; McCloskey, B. D.; Persson, K. A. Ion Transport and the True Transference Number in Nonaqueous Polyelectrolyte Solutions for Lithium Ion Batteries. *ACS Cent. Sci.* **2019**, *5*, 1250−1260.

(48) Williams, C. K.; Rasmussen, C. E. *Gaussian processes for machine learning*; MIT Press: 2006; Vol. 2.

(49) González, J. GPyOpt: A Bayesian Optimization framework in Python. http://github.com/SheffieldML/GPyOpt, accessed February 1, 2019.